Chemical- or Radiation-Assisted Selective Dealloying in Bimetallic Nanoclusters

G. Mattei,* G. De Marchi, C. Maurizio, P. Mazzoldi, C. Sada, and V. Bello
INFM, Dipartimento di Fisica, Università di Padova, via Marzolo 8, I-35131, Padova, Italy

G. Battaglin
INFM, Dipartimento di Chimica Fisica, Università di Venezia, Dorsoduro 2137, I-30123 Venezia, Italy
(Received 28 July 2002; published 25 February 2003)

A selective dealloying in bimetallic nanoclusters prepared by ion implantation has been found upon thermal annealing in oxidizing atmosphere or irradiation with light ions. In the first process, the incoming oxygen interacts preferentially with copper promoting Cu_2O formation, therefore extracting copper from the alloy. In the second process the irradiation with Ne ions promotes a preferential extraction of Au from the alloy, resulting in the formation of Au-enriched "satellite" nanoparticles around the original Au_xCu_{1-x} cluster.

DOI: 10.1103/PhysRevLett.90.085502 PACS numbers: 61.46.+w, 61.80.Jh, 81.05.Bx

Metal nanoclusters (NCs) embedded in insulating matrices have received an increasing interest in the last decade due to their peculiar optical, magnetic, and catalytic properties when the size becomes comparable to or less than the electronic mean free path [1–11]. Metallic NCs embedded in glass can increase the optical third-order susceptibility $\chi^{(3)}$ of the matrix by several orders of magnitude, making such systems interesting candidates to be used as optical switches [3,12]. With respect to the monoelemental case, when dealing with bimetallic nanoclusters one has an additional parameter to play with for controlling NCs properties, i.e., the composition. Of course, before the "tunability" of the NCs properties can be used for actual devices, a careful control over alloy clusters synthesis and stability has to be achieved, in order to clarify which are the parameters (i.e., implantation conditions, subsequent thermal or laser annealings, ion irradiation, etc.) that can promote separation (via oxidation, for instance) instead of alloying of the implanted species. Among different possible synthesis processing, ion-beam-based techniques proved to be very suitable in synthesizing NC-containing glasses [4,5,13–18]. Moreover, the composition of the clusters can be varied easily by sequential ion implantation in the matrix of two different elements, whose energy and dose can be tailored so as to maximize the overlap between the implanted species and to control their local relative concentration.

The aim of the present work is to present two possible paths for promoting an elemental-selective dealloying in bimetallic Au_xCu_{1-x} nanoclusters. Dealloying is usually described in terms of corrosion, as a selective dissolution of the most electrochemically active element of the alloy [19]. This process results in the formation of a nanoporous structure composed almost entirely of the more noble alloy constituent. As a room temperature (RT) process, dealloying is mainly assisted by the formation and migration of divacancies, which are known to diffuse faster than single vacancies at RT [20]. We will show that we can obtain also the inversion of this path (which is followed under chemically driven dealloying), therefore extracting preferentially the more noble metal (Au, in our case) from the alloy.

Fused silica (type II, Heraeus) slides were implanted with a 200 keV high-current Danfysik 1090 implanter at the INFN-INFM Implantation Laboratory (Legnaro, Italy). Au^+ and Cu^+ sequential implantations were performed at room temperature at a current density of 2 μA/cm^2, ion energies of 190 keV for Au and 90 keV for Cu and doses of 3×10^{16} ions/cm^2 for both ions. Implanted slides were then heat treated in a conventional furnace at 900 °C temperature in a H_2(4%)-N_2 atmosphere. This is the reference sample, in the following labeled as Au3Cu3H. Thermal annealing in air at 900 °C in a conventional furnace was performed for increasing time intervals, from 15 min up to 5 h. The reference samples were also ion irradiated with 190 keV Ne ions at a dose of 1×10^{17} ions/cm^2 and 2 μA/cm^2 of current density (with these irradiation conditions we measured a temperature increase lower than 50 °C in the sample, therefore ruling out a major effect of the temperature). Structural and compositional characterization was performed at CNR-IMM (Bologna, Italy) with a field-emission gun (FEG) Philips TECNAI F20 microscope operating at 200 kV equipped with an EDAX energy-dispersive x-ray spectrometer (EDS). Optical absorption spectra were collected with a CARY 5E UV-VIS-NIR dual beam spectrophotometer in the 200–800 nm wavelength range. Gold and copper concentration profiles were measured by 2.2 MeV $^4He^+$ Rutherford backscattering spectrometry (RBS).

In a previous paper concerning the formation of the Au_xCu_{1-x} alloy with sequential ion implantation and subsequent thermal annealing, we found that, upon annealing in reducing atmosphere, Au_xCu_{1-x} alloy nanoclusters, formed after sequential ion implantation, change their composition and grow, because of the Cu atoms (initially oxidized and dispersed in the matrix) reduced and incorporated in the clusters upon annealing,

resulting in a $Au_{0.5}Cu_{0.5}$ final composition [10]. We used those results to obtain relatively large Au_xCu_{1-x} alloy nanoclusters with a negligible amount of oxidized Cu. The size distribution of the clusters in these reference samples exhibits an average diameter $\langle D \rangle = 13.8$ nm and a standard deviation of the experimental bimodal distribution $\sigma = 11.7$ nm. An additional feature of the reference samples is the topological distribution of the clusters. As can be seen in Fig. 1(a), three distinct layers of well-separated spherical clusters are present: one at the surface, one at the projected range of the original sequential implantation (about 70 nm), and one at a depth of about 200 nm, i.e., the end of implantation damage [21].

A first attempt at obtaining a selective dealloying was carried out with thermal annealing in oxidizing (air) atmosphere. The TEM cross-sectional bright-field micrographs of the sample Au3Cu3H is shown in Figs. 1(a) and 1(b) before and after a thermal annealing in air at 900 °C for 15 min, respectively. The effect of the annealing is to extract Cu as Cu_2O (cuprite, cubic, $a = 0.4267$ nm) as a first step. Cu_2O is stabilized by the crystallographic cubic template of the Au_xCu_{1-x} alloy, as can be seen from the selected area electron diffraction (SAED) pattern of Fig. 1(c) obtained from the area indicated by the dashed circle in Fig. 1(b). In this image couples of "twin spots" aligned in the radial direction indicate two coherent cubic phases with the crystallographic axes aligned, which can be indexed as an Au-rich Au_xCu_{1-x} alloy ($x \sim 0.9$) and Cu_2O [in Fig. 1(d) the powder diffraction spectra of both phases are compared]. Further evidence of this interpenetrated structure can be obtained by EDS analysis. Scanning a 8 nm focused electron beam on different areas of the twofold clusters indicated by arrows in Fig. 1(b) a compositional variation across the cluster has been obtained as reported in Table I for the four points labeled in Fig. 1(b). We underline that the heat of formation of Cu_2O is about 167 ± 20 kJ/mol [22] to be compared to the corresponding value of AuCu alloy, 5.3 ± 0.5 kJ/mol.

It is interesting to note that if the annealing time interval is increased up to 5 h an asymptotic equilibrium is reached in which all the Cu atoms are extracted from the alloy and are driven at the sample surface where they are oxidized in large polycrystalline clusters of CuO [23] (tenorite, monoclinic, the most stable copper oxide). Therefore, as far as the thermal oxidation is concerned, the dealloying path follows a pattern similar to the corrosion process [19], in which the less noble (and more reactive element) is extracted from the alloy. We can reverse this picture by performing an irradiation of the alloy clusters with Ne ions at 190 keV. The effect is shown in Fig. 2(b) in comparison with the unirradiated reference Fig. 2(a).

The most evident result is the new topology of the clusters: around each original cluster a set of satellite clusters of about 1–2 nm are present with an average

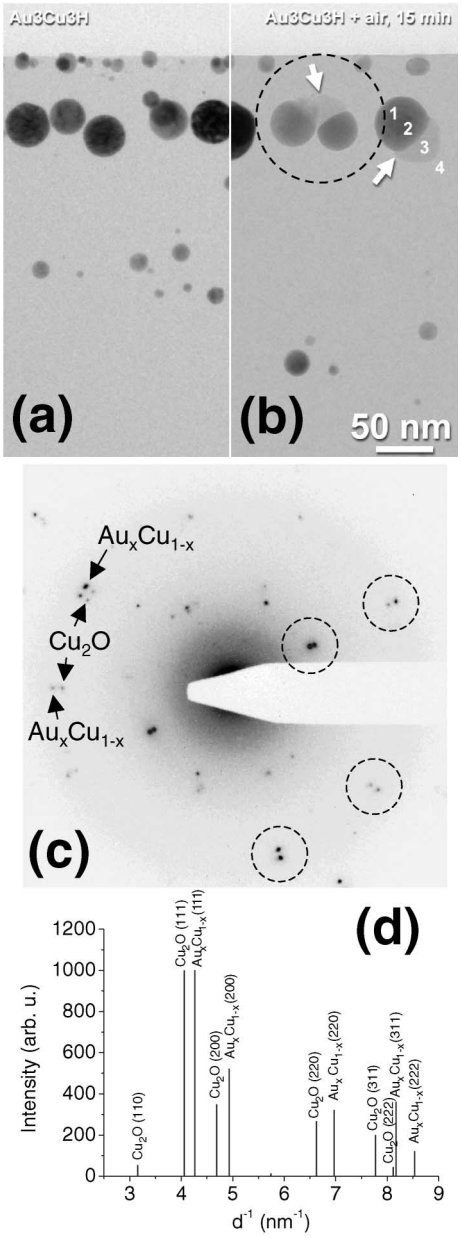

FIG. 1. Bright-field TEM cross-sectional micrograph of the sample Au3Cu3H [annealing in $H_2(4\%)$-N_2 atmosphere at 900 °C for 1 h] (a) before and (b) after a thermal annealing in air at 900 °C for 15 min. The arrows indicate some of the twofold clusters made of a Au-enriched alloy and Cu_2O; (c) SAED diffraction pattern from the circular region of part (b); (d) simulation of the diffraction pattern from Au_xCu_{1-x} alloy ($a = 0.406$ nm) and cubic Cu_2O in the cuprite phase ($a = 0.4267$ nm).

distance of about 3 nm from the cluster surface, similarly to what was reported in ion beam mixing experiments of Au islands irradiated by Au MeV ions [24–26]. In those works, the NC halo observed around the larger Au precipitates was explained in terms of the ballistic process, which dissolves NCs into the SiO_2 host by ion mixing, and of the large increase in the solute concentration in the

TABLE I. EDS compositional analysis at AuL and CuK edges on the sample annealed in air at 900 °C for 15 min.

Zone	Au/Cu	Phase	x
1	10.5 ± 0.3	Au_xCu_{1-x}	0.90 ± 0.06
2	2.0 ± 0.1	Au_xCu_{1-x}	0.66 ± 0.06
3	0 (only Cu)	Cu_2O	···
4	0 (no Au or Cu)	SiO_2	···

matrix with a subsequent precipitation. Simulations with the SRIM code [27] indicate that in those experiments the nuclear components of the energy loss (S_n) is comparable to the electronic one (S_e), whereas in the present work for 190 keV Ne ions the ratio S_e/S_n is about 3. Two points are worth noting in the present experiment. The first is the asymmetry in the density of the satellites around the clusters: a closer inspection of Fig. 2(c) shows that they are more dense and slightly larger in the region opposite to the surface (i.e., to the irradiating beam direction) with

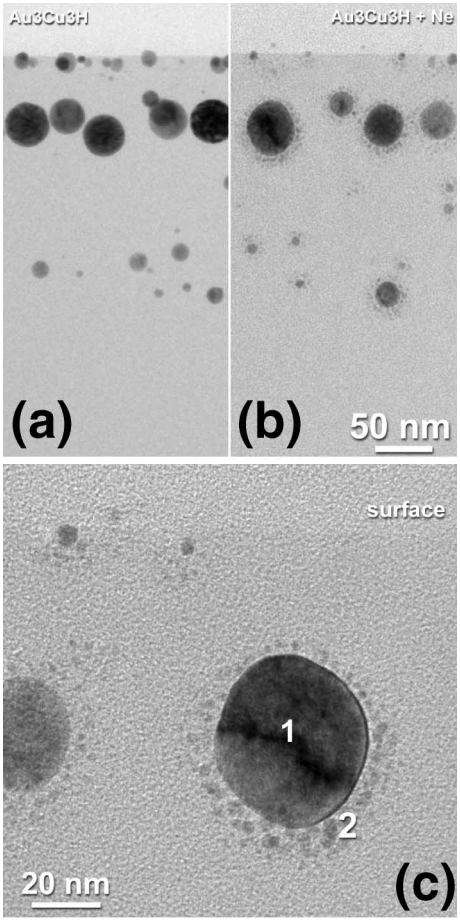

FIG. 2. Bright-field TEM cross-sectional micrograph of the sample Au3Cu3H [annealing in $H_2(4\%)$-N_2 atmosphere at 900 °C for 1 h] (a) before and (b) after irradiation at room temperature with 190 keV Ne ions, at a dose of 1×10^{17} ions/cm^2. In (c) the satellite-like topology of the clusters is shown at higher magnification.

respect to the cluster. The latter regards the composition of the satellites: EDS compositional analysis with a focused 2 nm electron beam of the FEG-TEM in the central part of the cluster [region one of Fig. 2(c)] gives an Au/Cu atomic ratio (measured at AuL and CuK lines) of 1.3 ± 0.1, whereas the same ratio measured in region 2 (i.e., on the satellite clusters) is 3.2 ± 0.3, indicating a preferential extraction of Au from the original clusters. The asymmetry in the satellite cluster density supports the hypothesis of a relevant contribution of the S_n components of the energy loss in the creation of an elemental-selective vacancy formation in the NCs, which could be also responsible for the preferential Au going out from the original alloy. Coulter and Parkin [28] derived an integrodifferential equation to calculate the number of displacements produced in a polyatomic target by a primary knock-on atom (PKA), on the basis of the Lindhard *et al.* method [29]. The net displacement damage function presents a similar form to the modified Kinchin-Pease function [30] introducing a displacement threshold for every type of atom. The calculated ratio of the displacement efficiencies is increasing with the ratio between the corresponding element mass. Replacement collision sequences may then influence the final state in a complex way. Moreover, preferential elemental ejection is correlated to different transport processes such as radiation enhanced diffusion, recoil implantation or cascade mixing, surface segregation, or radiation induced solute segregation. We observe that, on the basis of the Neumann-Kopp rule [22], in the bulk Au_xCu_{1-x} alloy for $x \sim 0.56$, as in the present case, the Au partial molar entalpy of formation ($\Delta H_{Au} = -236 \pm 20$ cal/g-atom) is higher than the corresponding Cu one ($\Delta H_{Cu} = -887 \pm 90$ cal/g-atom) [31], suggesting a possible preferential vacancy formation in the Au sublattice. This asymmetric behavior in the two sublattices can be also interpreted in terms of a deviation from the virtual crystal approximation recently demonstrated in AuCu alloys [32]. Additional effects of preferential (Au) elemental segregation [33], which may be relevant in medium-large size clusters, can give further driving force to the dealloying mechanism via Au extraction. The extracted gold atoms tend to precipitate as a consequence of the radiation enhanced diffusion and of the local overcoming of the solubility limit [34]. A more quantitative investigation of the nuclear component effect of this elemental-selective dealloying is in progress by varying the irradiating ions, at constant energy and released power density, and the composition of the irradiated alloy NCs [35]. Preliminary results on irradiation with He, Ne, or Kr ions of AuAg alloy nanoclusters in SiO_2 completely corroborate in a quantitative way the picture for dealloying proposed in the present Letter, i.e., that a similar preferential segregation of Au in the satellite clusters is found. This is a confirmation that the mechanism proposed in the present Letter is of general validity and independent of the

particular system investigated. Moreover, a clear direct correlation between the size of the satellite clusters and the nuclear component of the energy released by the incoming ions is found.

Optical absorption measurements in the present Ne-irradiated AuCu samples indicate a redshift of the surface plasma resonance (SPR) from 550 to 575 nm, which would correspond to the SPR of pure Cu clusters. Therefore, as the actual cluster composition measured by EDS is roughly comparable to the original one, this is an indication that we cannot interpret this shift merely in terms of a compositional change and that we have to consider that the topological arrangement of the satellites clusters, about 2–3 nm from the original cluster surface, can induce a strong coupling, which cannot be accounted for by a simple Mie-type theory [12,35].

In conclusion, we presented two different experimental approaches for an elemental-selective dealloying of bimetallic Au_xCu_{1-x} nanoclusters in dielectic matrix. The first dealloying process (induced by thermal annealing in oxidizing atmosphere) follows a path similar to the corrosion process, in which the less noble element (Cu, in the present case) is extracted by its chemical interaction with the incoming oxygen. On the contrary, in the latter mechanism, vacancy formation sustained by ballistic process during Ne irradiation produces the Au preferential going out in a peculiar topological arrangement, in which small satellites nanoparticles surround the original alloy cluster. In both cases a crucial role is played by vacancy formation and diffusion, giving a unified interpretative framework. Work is in progress to better elucidate the contribution of the ion deposited energy and the thermodynamic aspects in the dealloying process during ion irradiation.

We gratefully acknowledge the technical assistance of M. Parolin at Ion Implantation Laboratory (Legnaro, Italy).

*Corresponding author.
Email address: mattei@padova.infm.it

[1] F. Gonella and P. Mazzoldi, *Handbook of Nanostructured Materials and Nanotechnology* (Academic Press, San Diego, 2000), Vol. 4, Chap. 2, p. 81.
[2] H. Hosono, Phys. Rev. Lett. **74**, 110 (1995).
[3] P. Mazzoldi, G.W. Arnold, G. Battaglin, F. Gonella, and R. Haglund, Jr., J. Nonlinear Opt. Phys. Mater. **5**, 285 (1996).
[4] G. Battaglin, Nucl. Instrum. Methods Phys. Res., Sect. B **116**, 102 (1996).
[5] F. Gonella, Nucl. Instrum. Methods Phys. Res., Sect. B **166–167**, 831 (2000).
[6] E. Cattaruzza, Nucl. Instrum. Methods Phys. Res., Sect. B **169**, 141 (2000).
[7] R. H. Magruder III, J. E. Wittig, and R. A. Zuhr, J. Non-Cryst. Solids **163**, 162 (1993).
[8] R. H. Magruder III, D. H. Osborne, Jr., and R. A. Zuhr, J. Non-Cryst. Solids **176**, 299 (1994).
[9] E. Cattaruzza *et al.*, Nucl. Instrum. Methods Phys. Res., Sect. B **148**, 1007 (1999).
[10] F. Gonella, G. Mattei, P. Mazzoldi, C. Sada, G. Battaglin, and E. Cattaruzza, Appl. Phys. Lett. **75**, 55 (1999).
[11] G. Mattei, Nucl. Instrum. Methods Phys. Res., Sect. B **191**, 323 (2002).
[12] U. Kreibig and M. Vollmer, *Optical Properties of Metal Clusters* (Springer-Verlag, Berlin, 1995).
[13] G.W. Arnold and J. A. Borders, J. Appl. Phys. **48**, 1488 (1977).
[14] N. Skelland and P. Townsend, Nucl. Instrum. Methods Phys. Res., Sect. B **93**, 433 (1994).
[15] N. Skelland and P. Townsend, J. Non-Cryst. Solids **188**, 243 (1995).
[16] C. White, J. Budai, J. Zhu, S. Withrow, D. Hembree, D. Henderson, A. Ueda, Y. Tung, and R. Mu, Mater. Res. Soc. Symp. Proc. **396**, 377 (1996).
[17] A. Meldrum, L. Boatner, and C. White, Nucl. Instrum. Methods Phys. Res., Sect. B **178**, 7 (2001).
[18] E. Valentin, H. Bernas, C. Ricolleau, and F. Creuzet, Phys. Rev. Lett. **86**, 99 (2001).
[19] J. Erlebacher, J. M. Aziz, A. Karma, N. Dimitrov, and K. Sieradzki, Nature (London) **410**, 450 (2001).
[20] R.W. Cahn, Nature (London) **389**, 121 (1997).
[21] G.W. Arnold, G. Battaglin, A. Boscolo-Boscoletto, F. Caccavale, G. De Marchi, and P. Mazzoldi, Mater. Res. Soc. Symp. Proc. **235**, 407 (1992).
[22] *Metals Reference Book*, edited by C. Smithells and E. Brandes (Butterworths, London, 1976).
[23] G. Battaglin *et al.*, Nucl. Instrum. Methods Phys. Res., Sect. B **175–177**, 410 (2001).
[24] J. C. Pivin and G. Rizza, Thin Solid Films **366**, 284 (2000).
[25] J. C. Pivin, Mater. Sci. Eng. A **293**, 30 (2000).
[26] G. Rizza, M. Strobel, K. H. Heining, and H. Bernas, Nucl. Instrum. Methods Phys. Res., Sect. B **178**, 78 (2001).
[27] J. F. Ziegler, J. P. Biersack, and U. Littmark, *The Stopping and Range of Ions in Solids* (Pergamon, New York, 1985).
[28] *Ion-Solid Interactions: Fundamentals and Applications*, edited by M. Nastasi, J.W. Mayer, and J. K. Hirvonen (Cambridge University Press, Cambridge, United Kingdom, 1996).
[29] J. Lindhard, V. Nielsen, M. Scharff, and P. Thomsen, Mat. Fys. Medd. K. Dan. Vidensk. Selsk. **33** (1963).
[30] G. Kinchin and R. Pease, Rep. Prog. Phys. **18**, 1 (1955).
[31] R. Hultgren, R. L. Orr, P. Anderson, and K. K. Kelley, *Selected Values of Thermodynamic Properties of Metals and Alloys* (John Wiley and Sons, Inc., New York, 1963).
[32] A. I. Frenkel, V. S. Machavariani, A. Rubshtein, Y. Rosenberg, A. Voronel, and E. A. Stern, Phys. Rev. B **62**, 9364 (2000).
[33] S. M. Foiles, M. I. Baskes, and M. S. Daw, Phys. Rev. B **33**, 7983 (1986).
[34] A. Miotello, G. De Marchi, G. Mattei, P. Mazzoldi, and C. Sada, Phys. Rev. B **63**, 075409 (2001).
[35] G. Mattei, V. Bello, G. De Marchi, P. Mazzoldi, and C. Sada (to be published).